CPC(HEP & NP), 2010, **34**(10): 1649–1654 Chinese Physics C Vol. 34, No. 10, Oct., 2010

A proposed method to characterize high harmonic microbunching in EEHG operation of SDUV-FEL*

DENG Hai-Xiao(邓海啸)[1)]

Shanghai Institute of Applied Physics, Chinese Academy of Sciences, Shanghai 201800, China

Abstract The echo-enabled harmonic generation (EEHG) scheme offers remarkable efficiency for generating high harmonic microbunching with a relatively small energy modulation. A proof of principle experiment of the EEHG scheme has been proposed at the Shanghai deep ultraviolet (SDUV) free electron laser (FEL) facility, where the 4th harmonic of the seed laser is amplified in the 9 m long radiator. To explore the advantages of the EEHG scheme, in this paper, a method of measuring the coherent high harmonic radiation of the radiator is proposed to investigate the electron beam microbunching corresponding to the 10th–20th harmonics of the seed laser. The principle of the proposed method, comparisons with existing methods and the simulation results are presented and discussed.

Key words harmonic, microbunching, coherent transition radiation, coherent harmonic radiation

PACS 41.60.Cr

1 Introduction

On the way to compact and fully temporal coherent radiation sources in the short-wavelength spectral region, in the free electron laser (FEL) community, several double modulator schemes [1–4] are proposed to improve the frequency up-conversion efficiency of the standard high gain harmonic generation (HGHG) FEL. Among them, the echo-enabled harmonic generation (EEHG) scheme exhibits unprecedented frequency up-conversion efficiency and allows for the generation of ultra-high harmonics with relatively small energy modulation. It is found that the Shanghai deep ultraviolet (SDUV) [5] FEL is well suited to the EEHG scheme with only minor modifications. Thus, a proof-of-principle experiment of the EEHG scheme has been proposed at SDUV-FEL [6].

The current layout of the double modulator section of SDUV-FEL is illustrated in Fig. 1. The original laser injection chicane is redesigned to produce larger R_{56} and one more laser injection port is added near the linac exit. The 1048 nm seed laser is split into two beams for the two modulators. Since the beam energy is 160 MeV and the existing 9 m long radiator is designed to be resonant at the 4th harmonic of the 1048 nm seed laser pulse, it is determined to first operate the EEHG scheme at the 4th harmonics of the seed laser. Thus the radiation with a 262 nm wavelength is planned to be amplified in the radiator.

However, the most attractive feature of the EEHG scheme is the efficient generation of high harmonic microbunching with relatively small energy modulation. Intensive studies [7] indicate that for the 4th harmonic generation in SDUV-FEL, the EEHG scheme results in similar performance when compared with other double modulator schemes [1, 2], which is a little bit better than that of the standard HGHG scheme. Thus, in order to explore the promising ability of the EEHG technique at high order harmonics, the characterization of high harmonic microbunching in the EEHG scheme has recently been under consideration.

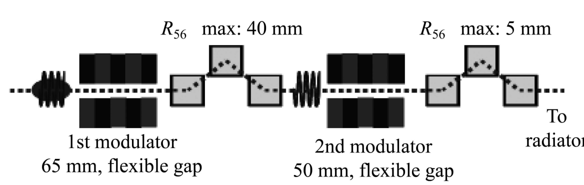

Fig. 1. The double modulator section of SDUV-FEL.

Received 11 September 2009

* Supported by Shanghai Natural Science Foundation (09JC1416900)

1) E-mail: denghaixiao@sinap.ac.cn

Since there is no available resonant radiator for high harmonics of the seed laser, these high harmonics cannot be amplified to saturation in SDUV-FEL. It seems that high harmonic microbunching can only be measured at the exit of the second chicane by some longitudinal diagnoses, i.e., coherent transition radiation (CTR) and coherent synchrotron radiation (CSR), etc. In this paper, a novel method based on coherent harmonic radiation (CHR) in the radiator is proposed to picture the high harmonic microbunching of the electron beam in the EEHG operation of SDUV-FEL. It shows that the CHR-based method is more convenient and robust when compared with the conventional CTR-based one. We first briefly describe the principle of the CHR-based measurement in Section 2. Then, on the basis of SDUV-FEL parameters, the simulation performance of the CHR is illustrated in Section 3. Preliminary concepts on the extraction and measurement of the CHR are discussed in Section 4. Finally, we present our conclusions in Section 5.

2 Principles and comparisons of CTR and CHR

One of the most popular longitudinal beam diagnoses is the CTR-based method, which relies on the fact that the coherent radiation spectrum emitted by the electron beam as it passes a transition foil is essentially the Fourier transform of the longitudinal beam distribution. This has been widely used in diagnosing macrobunches at the picosecond level [8, 9]. In recent years, the CTR-based method was dramatically driven by FEL applications. It has been successfully used to measure the electron beam microbunching in FEL [10–12] and inverse FEL processes [13–15]. If the microbunched beam is taken to be

$$f(x,y,z) = \frac{N_{\mathrm{b}}}{(2\pi)^{3/2}\sigma_x\sigma_y\sigma_z}\mathrm{e}^{-\frac{x^2}{2\sigma_x^2}-\frac{y^2}{2\sigma_y^2}-\frac{z^2}{2\sigma_z^2}} \times\left[1+\sum_{n=1}^{\infty}b_n\sin(nk_{\mathrm{r}}z)\right], \quad (1)$$

where N_{b} is the number of electrons in the bunch, $\sigma_{x,y,z}$ are the transverse (x, y) and longitudinal (z) beam sizes, respectively, k_{r} is the radiation wave number (and thus the beam modulation wave number), n is the harmonic number and b_n is the microbunching factor for the n^{th} harmonic. If one assumes that the microbunching period in the beam's rest frame is much smaller than the transverse beam size, i.e., $k_{\mathrm{r}}\sigma_{x,y}/\gamma \gg 1$, which is indeed the case for a FEL, the nth harmonic CTR energy emitted when the electron beam strikes a conducting surface can be given as [10]

$$U_n = \frac{nhc\alpha(N_{\mathrm{b}}b_n)^2}{8\pi^{3/2}\sigma_z}\left(\frac{\gamma}{nk_{\mathrm{r}}}\right)^4\left(\frac{\sigma_x^2+\sigma_y^2}{\sigma_x^3\sigma_y^3}\right), \quad (2)$$

where α is the fine structure constant, h is the Planck constant, c is the speed of light in vacuum and γ is the mean electron beam energy in unit of m_0c^2. It is noted that higher charge intensities, higher microbunching and smaller beam size would enhance CTR production.

High harmonics of the undulator radiation are regarded as a natural extension to short wavelengths [16–18], and of great interest. According to the well-known FEL physics, harmonic evolution in an undulator can be written as

$$\frac{\partial}{\partial z}E_m(z) = \frac{eK[JJ]_m}{4\gamma m_0c^2}b_m(z), \quad (3)$$

where m is the harmonic order of undulator radiation, E_m is the slowly varying envelope of the radiation field, e is the charge of a single electron, K is the dimensionless undulator parameter and $[JJ]_m$ is the polarization factor for planar undulator.

In the EEHG scheme, by adjusting the seed laser and the dispersion of chicanes, the electron beam density can be efficiently modulated on arbitrary harmonics of the seed laser. In other words, the EEHG scheme performs significant microbunching for the selected harmonic, while other harmonics still preserve the noise level. Thus, if the longitudinal density modulation of the electron beam is optimized at the 12th or 20th harmonic of the seed laser in the EEHG operation, i.e. the 3rd or 5th order harmonic of the planar radiator in SDUV-FEL, strong CHR signals would be observed at the beginning of the radiator. For a microbunched electron beam as Eq. (1) in the EEHG operation of SDUV-FEL, the CHR power of the mth harmonic radiation of the radiator reads

$$P_m = \frac{\int|E_m(r)|^2\mathrm{d}^2r}{2Z_0} = \frac{Z_0(IKb_m[JJ]_ml)^2}{12\pi(\sigma_x^2+\sigma_y^2)\gamma^2}. \quad (4)$$

And the CHR energy of the mth harmonic radiation yields

$$U_m = \frac{Z_0(IKb_m[JJ]_ml)^2\sigma_z}{5\pi(\sigma_x^2+\sigma_y^2)\gamma^2c}, \quad (5)$$

where I is the peak current of the electron beam and l is the passed radiator length.

Since SDUV-FEL employs 2 pop-in monitors in each radiator segment for beam and laser diagnoses, this strong CHR can be reflected by the pop-in mirror for further measurement. In comparison with the

CTR based characterization for high harmonic microbunching in the EEHG operation of SDUV-FEL, the following prospects arise from the CHR-based method.

1) The radiation energy of CHR is much larger than that of CTR, which is helpful in improving the sensitivity of high harmonic microbunching measurements. Here we consider the 3rd harmonic radiation of the radiator as an example, i.e., n=12 and m=3. We assume an electron beam with transverse beam size of $\sigma_{x,y}$=200 μm, beam charge of 0.75 nC and longitudinal beam size of σ_z=300 μm. After the density modulation by the 1048 nm seed pulse, the corresponding electron beam microbunching b_{12} is 0.10. Then with a radiator length of l=0.1 m, according to Eqs. (2) and (3), the estimated 87.3 nm radiation energy from CTR and CHR is about 130 fJ and 4 nJ, respectively. Therefore, the radiation energy from CHR is 3×10^4 times the CTR.

2) The spectrum of CHR is much purer than that of CTR. The radiation spectrum of CHR only appears at the first several harmonics of the radiator radiation and dominates in the interested harmonic. In our case, the maximum signal is the 3rd harmonic of the radiator, and the main noise source is the fundamental of the radiator, i.e., 262 nm radiation, where b_4=0.003 will exhibit a radiation energy of 40 pJ. In contrast, CTR has a broad spectrum, especially at each harmonic of the seed laser. Since there is a correlation of $1/n^3$, the fundamental and the lower harmonics have much larger radiation energy with respect to the concerned 12th harmonic of the seed laser. This means that, in the diagnosis, the radiation source from CHR has a better signal noise ratio than that of CTR.

3 Simulation results

In this section, we numerically investigate the CHR in the EEHG operation of SDUV-FEL. The FEL simulation is performed with GENESIS [19], which has been widely used in the simulations of many FEL projects around the world. The simulation consists of three runs. In the first run, the energy modulation from the 1048 nm seed laser in Modulator 1 is simulated and the particle distribution is dumped at the exit of Modulator 1. The macroparticles are imported, transported through DS 1 and further sent to Modulator 2 for the second energy modulation. At the exit of Modulator 2, the particle distribution is dumped again. Finally, the macroparticles are re-imported for the third run, where the radiator is tuned to the 4th harmonic of the seed laser, i.e. 262 nm.

Table 1. Parameters of SDUV-FEL with the EEHG scheme.

parameters	value
electron beam energy	160 MeV
peak current	0.3 kA
normalized emittance	6 μm·rad
local energy spread	1×10^{-4}
seed laser wavelength	1048 nm
seed laser duration	10 ps
seed laser waist	0.7 mm
seed laser 1 power	5 MW
seed laser 2 power	2 MW
$R_{56}^{(1)}$	7.0 mm
$R_{56}^{(2)}$	0.6 mm
modulator 1 period length	65 mm
modulator 1 periods	10
modulator 2 period length	50 mm
modulator 2 periods	10
radiator period length	25 mm
radiator parameter K	1.45

We consider the 12th harmonic of the 1048 nm seed laser, i.e., 87.3 nm. With the parameters listed in Table 1, the longitudinal beam density modulation is optimized at the 12th harmonic of the seed laser when entering the radiator. The bunching factor versus the harmonic number is shown in Fig. 2, where b_{12}=0.10 is clearly displayed. Meanwhile, b_1=0.07 and b_4 = 0.003 are observed.

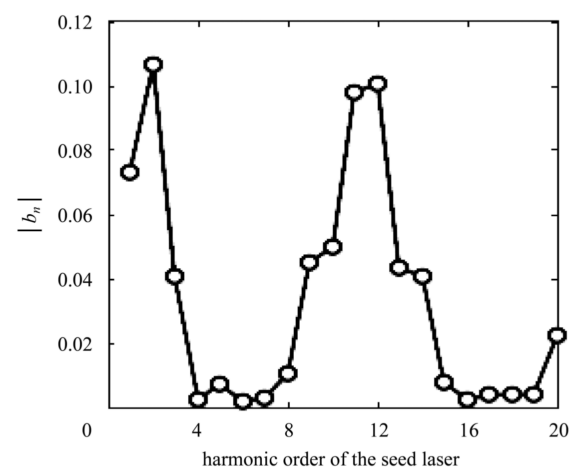

Fig. 2. The bunching factor versus the harmonic number.

The 3rd harmonic energy of the radiator radiation is clearly enhanced by the EEHG operation in SDUV-FEL. As seen in Fig. 3, the large microbunching factor favored by the EEHG scheme is responsible for the initial significant growth of the 87.3 nm radiation energy. Finally, at the radiator position of the extracting point, the 3rd 87.3 nm CHR energy exceeds 7.5 nJ while the 5th CHR 52.4 nm radiation energy is 0.2 nJ, which is basically consistent with the analytical results presented in the previous section. However, the fundamental radiation reaches the energy of 2.4 nJ, which is much larger than the theoretical estimate. This phenomenon is due to the complex transverse distribution of the electron beam microbunching, which was not taken into account in Eqs. (3)–(5) but in numerical simulations. If the transverse features of the electron beam microbunching are considered, Eq. (4) will be rewritten as

$$P_m \propto \int |I(r)b_m(r)|^2 \mathrm{d}^2 r. \tag{6}$$

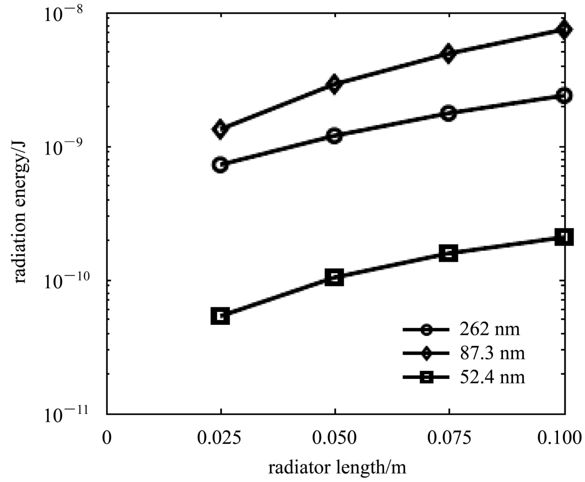

Fig. 3. The growth of the CHR energy in the radiator.

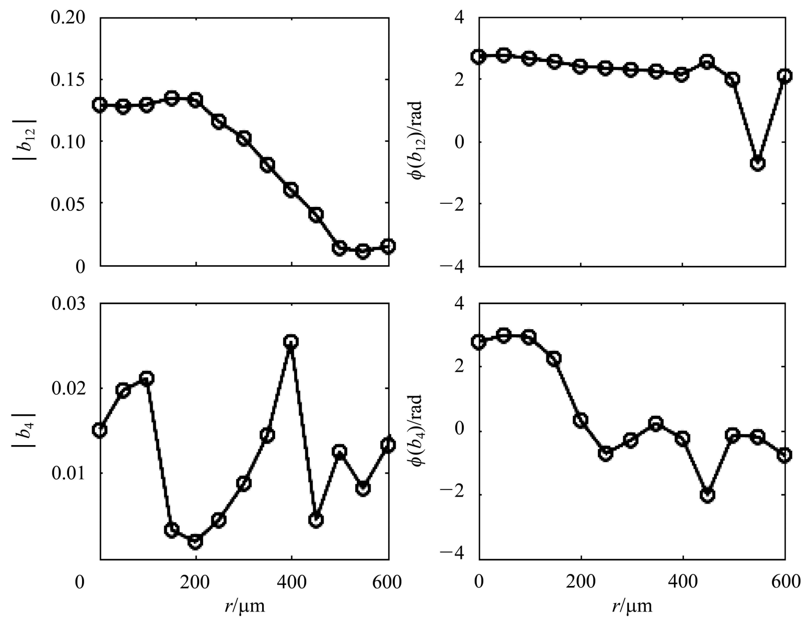

Fig. 4. Transverse features of the electron beam microbunching.

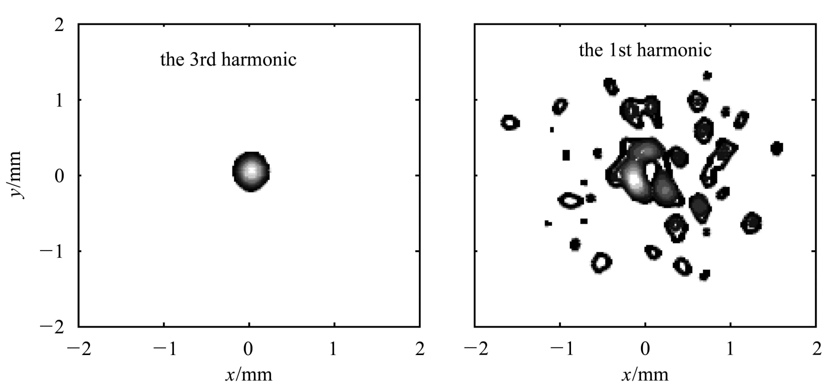

Fig. 5. Transverse distributions of the CHR in the radiator.

The simulation results of the radial distribution of the electron beam microbunching are shown in Fig. 4. For the interested 3rd harmonic of the radiator radiation, most of the electrons at different radial positions are modulated on the same pattern, which presents a similar angle of the electron beam microbunching. For the 1st harmonic of the radiator radiation, the electron beam shows the opposite bunching angle along the radial position and results in a much lower global microbunching than the local microbunching. Under such circumstances, the fundamental radiation emits much more energy than the theoretical estimation given by Eq. (5).

In order to clearly visualize what we have discussed above, the spatial distributions of the 3rd and 1st CHR are plotted in Fig. 5, where different transverse coherence of the 3rd and 1st harmonic strongly supports our statement. It reminds us that an appropriate observation aperture will be helpful in enhancing the signal to noise ratio in real experiments.

Figure 6 shows the radiation spectrum of the CHR at the first pop-in monitor in the SDUV-FEL radiator. The spectral characters of the CHR discussed above are confirmed. Thus, the radiator is utilized as a radiation amplifier and spectrum filter in the CHR-based method.

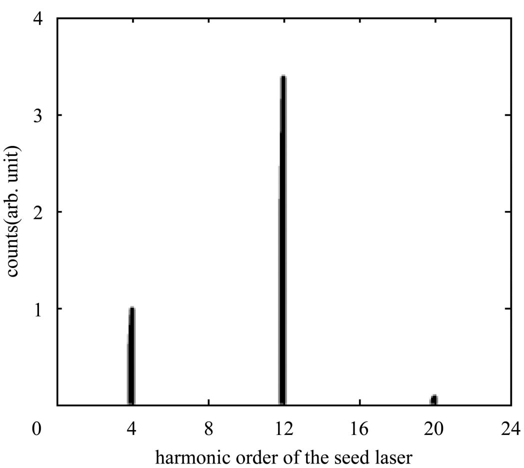

Fig. 6. The radiation spectrum at the extracting point.

4 Proposed measurement of CHR

The CHR can be reflected by the first pop-in mirror in the radiator, and sent to the further detectors. Since the 3rd harmonic 87.3 nm radiation and the 5th harmonic 52.4 nm radiation have already stepped into the vacuum ultraviolet spectral region, an in-vacuum system is designed to measure the CHR signal.

As shown in Fig. 7, the extracted output radiation is split into two parts. We attempt to measure the radiation energy and the radiation spectrum of the CHR. Since the energy of the interested high harmonic of the seed laser is about 7.5 nJ and dominant in the extracted radiation, a commercially available photodiode detector responding from the infrared to the X-ray spectral region can be used to measure the radiation energy of the interested CHR. The second part of the extracted radiation beam enters in a spectrometer, formed by one sphere grating and charge couple device (CCD), where the radiation spectrum of the CHR is obtained by a single shot method.

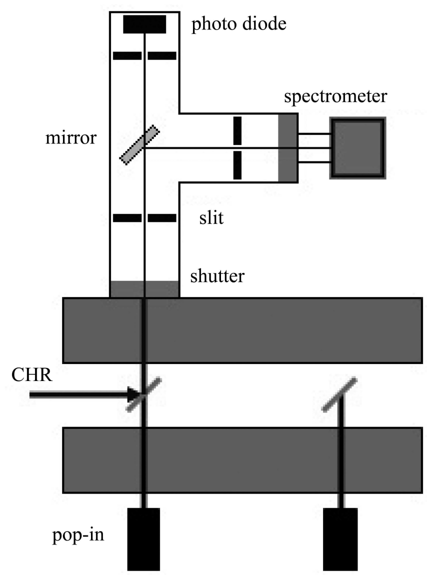

Fig. 7. The in-vacuum diagnostic system for CHR.

5 Conclusions

In this paper, a method to characterize high harmonic microbunching of the electron beam in the EEHG operation of SDUV-FEL is proposed, which is on the basis of the coherent high harmonic radiation in the existing radiator. In comparison with the conventional CTR-based method, the CHR in the radiator produces extremely strong radiation energy and a pure radiation spectrum. It is very helpful in improving the resolution and sensitivity of the diagnoses. A three dimensional simulation for the 12th CHR of the 1048 nm seed laser was carried out to illustrate the principle of the CHR-based method. After density modulation, the electron bunch enters the radiator with b_4=0.003 and b_{12}=0.10, then the radiation with U_4=2.4 nJ and U_{12}=7.5 nJ are modeled at the radiator position of the first pop-in system. An alternative case for the 20th CHR of the seed laser has also been studied, where the double modulator section parameters are chosen to optimize the density modulation of the electron beam at the 5th harmonic of the radiator resonant frequency. Then the CHR with energy of U_4=2.3 nJ, U_{12}=0.6 nJ and U_{20}=1.4 nJ is modeled.

In this proposal, the radiation is directly sent to the further detectors. In order to upgrade the performance, silicon plated mirror [20, 21] can be adopted as the harmonic separator of the 3rd and 5th harmonic radiation from the fundamental in the radiator. This separator can absorb most of the energy of the fundamental radiation by virtue of Brewster incidence at a special angle, while it can reflect the harmonics due to its small refractive index for XUV light. Moreover, the CHR intensity can be further enhanced by passing more radiator periods, and it can be detected at the second pop-in system in the radiator or even after one segment of radiator.

Generally, the CHR-based method is only applicable to the harmonics of the radiator resonant frequency. It is the 12th and 20th harmonic of the seed laser in the SDUV-FEL case. However, by using a harmonic operation technique [22], it can be extended to the 10th, 11th, 13th and so on. Moreover, the CHR-based approach is also applicable to the EEHG operation of the Shanghai soft X-ray FEL [23] case, in which the microbunching of the 30th harmonic of the 270 nm seed laser pulse can be characterized by the 5th harmonic radiation from the 1st stage radiator resonant at 45 nm.

References

1 Allaria E, Ninno G D. Phys. Rev. Lett., 2007, **99**: 014801

2 Jia Q K. Appl. Phys. Lett., 2008, **93**: 141102

3 Stupakov G. Phys. Rev. Lett., 2009, **102**: 074801

4 Xiang D. Stupakov G. Phys. Rev. ST Accel. Beams, 2009, **12**: 030702

5 ZHAO Z T, DAI Z M, ZHAO X F et al. Nucl. Instrum. Methods Phys. Res. A, 2004, **528**: 591

6 CHEN J H, DENG H X, GU Q et al. Chin. Phys. C, 2009, **33**: 706

7 YAN J, FENG C, CHEN J H et al. Proceeding of FEL09, UK, Liverpool, 2009; 406–409

8 Happek U, Sievers A J, Blum E B. Phys. Rev. Lett., 1991, **67**: 2962

9 Yukio Shibata et al. Phys. Rev. E, 1994, **50**: 1479

10 Tremaine A, Rosenzweig J B, Anderson S et al. Phys. Rev. Lett., 1998, **81**: 5816

11 Lumpkin A H, Dejus R, Berg W J et al. Phys. Rev. Lett., 2001, **86:** 79

12 Lumpkin A H, Arnold N D, Berg W J et al. Nucl. Instrum. Methods Phys. Res. A, 2001. **475**: 476

13 LIU Y, WANG X J, Cline D B et al. Phys. Rev. Lett., 1998, **80**: 4418

14 Sears C M S, Colby E, Ischebeck R et al. Phys. Rev. ST Accel. Beams, 2008, **11**: 061301

15 Tochitsky S Ya, Williams O B, Musumeci P et al. Phys. Rev. ST Accel. Beams, 2009, **12**: 050703

16 Bonifacio R, de Salvo L, Pierini P. Nucl. Instrum. Methods Phys. Res. A, 1990, **293:** 627–629

17 HUANG Z, Kim K J. Phys. Rev. E, 2000, **62:** 7295

18 Freund H P, Biedron S G, Milton S V. Nucl. Instrum. Methods Phys. Res. A, 2000, **445:** 53

19 Reiche S et al. Proceeding of PAC07. Albuquerque, New Mexico, USA: 2007, 1269–1271

20 Takahashi E J, Hasegawa H, Nabekawa Y et al. Opt. Lett., 2004, **29**: 507

21 Shimizu T, Okino T, Furusawa K et al. Phys. Rev. A, 2007, **75**: 033817

22 DENG H X, DAI Z M. Chin. Phys. C, 2008, **32**: 593

23 XIANG D, Stupakov G. SLAC-PUB-13475, 2008